

Optimizing Crop Yield Prediction in Precision Agriculture with Hyperspectral Imaging-Unmixing and Deep Learning

Dr. Deeba K^{1*}, Dr. O. Rama Devi², Dr. Mohammed Saleh Al Ansari³, Dr. Bhargavi Peddi Reddy⁴,
Dr. Manohara H T⁵, Prof. Ts. Dr. Yousef A. Baker El-Ebiary⁶, Manikandan Rengarajan⁷

Assistant Professor, School of Computer Science and Applications, REVA University, Bangalore¹

Professor and HOD, Department of AI and DS, Lakireddy Balireddy College of Engineering, Mylavaram, Vijayawada²

Associate Professor, College of Engineering-Department of Chemical Engineering, University of Bahrain, Bahrain³

Associate Professor, Dept of CSE, Vasavi College of Engineering, Hyderabad, India⁴

Assistant Professor, Department of Electronics and Communication Engineering,
NITTE Meenakshi Institute of Technology, Bengaluru⁵

Faculty of Informatics and Computing, UniSZA University, Malaysia⁶

Vel Tech Rangarajan Dr. Sagunthala R and D Institute of Science and Technology, Avadi, Chennai, Tamil Nadu, India-600062⁷

Abstract—The optimization of crop yield projections has arisen as a major problem in modern agriculture, due to the increasing demand for food supply and the necessity for effective resource management. Precision and scalability are hampered by the limits associated with conventional agricultural production prediction techniques, which mostly rely on observations and simple data sources. While methods like random forest (RF) and K-nearest neighbors (KNN) are widely used, their reliance on personal assessments and insufficient knowledge of crop attributes typically results in less accurate forecasts and makes them unsuitable for agricultural precision. The suggested method combines deep learning, spectral unmixing, and hyperspectral imaging methods to overcome these obstacles. With the use of hyperspectral imaging, which records a vast array of data that is not visible to the human eye, crop attributes may be thoroughly examined and can identify the unique spectral fingerprints of different agricultural constituents by using spectral unmixing approaches, which makes it easier to evaluate the health and growth phases of the crop. Then, using this augmented spectral data, deep learning algorithms create a solid, data-driven basis for precise crop production prediction. MATLAB has been used in the suggested workflow. The combination of deep learning, spectrum unmixing, and hyperspectral imaging provides a comprehensive, cutting-edge approach that goes beyond the constraints of conventional techniques were implemented in python. Some of the algorithms that were examined, this one with integration has the lowest Root Mean Square Error (RMSE) of 0.15 and Mean Absolute Error (MAE) of 0.14, demonstrating higher prediction accuracy above other current models. This novel method represents a substantial breakthrough in precision agriculture while also improving crop production prediction.

Keywords—Crop yield prediction; hyper spectral image; spectral unmixing; resource management; precision agriculture

I. INTRODUCTION

Demand for premium agricultural products will increase exponentially as people's standard of living rise. The amount of farmland has, regrettably, decreased due to environmental harm. Therefore, to meet increasing need for food, livestock

and agricultural producing operations have become more importance. With the goal of reducing the financial and environmental costs associated with food production, precision agriculture is a technique for boosting productivity [1]. Crop conditions are measured using remote sensing, which is subject to large variation. In order to manage resources and make judgments on crop development, agriculturalists need to have equipment that is technologically advanced. By giving information on crop health and development phases, hyperspectral photography facilitates targeted farming by allowing for effective insect and herbicide treatments. Globally, there is a growing need for modern technology, namely multispectral and hyperspectral pictures, to increase farming precision and control [2]. The hyperspectral images are able to distinguish between artefacts and physicals in a wide range of application fields, including precise agriculture, minerals recognition, analysis of the environment, and urban development [3].

Agriculture and forestry are anticipated to hold the biggest market share among other end-user sectors in the hyperspectral imagery industries. Hyperspectral imaging is utilized in farming and forestry for a number of tasks, including weed mapping, plant recognition, seed yield analysis, and forest management [4]. In addition, over the past ten years, sensors have collected an increasing amount of data on farms. Therefore, offers for data optimization as well as apps for farmers have been coordinated by hyperspectral service providers [5]. Key elements of successful agriculture include the monitoring of nutrient crops, water stress, disease, pest infarction, and general plant health. By using conventional optical detection methods like imaging or spectroscopy, it is difficult to guarantee adequate spatial and spectrum data for the analysis of food and agriculture harvests [6]. The limitations of conventional imaging approaches for sorting vegetables and fruit include their inability to separate internal from exterior product structures and to collect spectral information. The commonly used systems imitate human vision using colour video cameras; nevertheless, these approaches are costly, time-

consuming, and frequently result in sample obliteration. Furthermore time-consuming, costly, and sometimes obliterative, current procedures make it challenging to find product flaw [7].

Due to the rapid development of information science, image analysis, and precision agriculture over the past few years, optical detectors have developed into scientific tools. Particularly, the incorporation of a strategy to produce a spectral variation spatial map has led to substantial study and development in imaging and spectroscopic techniques, which has contributed to several well-liked applications in agriculture [8]. Precision agricultural methods have expanded and been more widely used as a result of the development of airborne and ground-based hyperspectral and multispectral imagery equipment. Along with its predictive skills, this technology has made it possible to characterize soils and vegetative cover, evaluate crop pressures, identify bruises in fruits and vegetables and estimate yield [9]. Hyperspectral and multispectral images provide a number of benefits, including inexpensive prices (in comparison to traditional scouting), reliable, simple use, rapid, non-destructive, extremely precise assessments, and a wide range of usages. Typical spectral images are made up of a number of monochromatic images that represent various wavelengths [10]. In comparison to traditional computer vision as well as human perception, hyperspectral imaging systems offer a natural advantage. Using hyperspectral imaging systems, any appearance features that are challenging or difficult to extract with systems may be retrieved [11]. A significant use for hyperspectral imaging is the assessment of the overall quality of agricultural and food items.

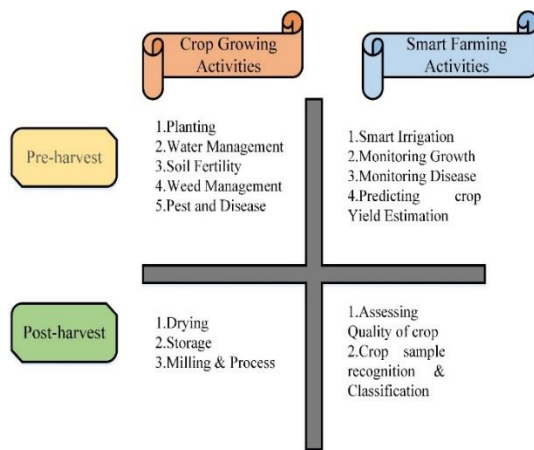


Fig. 1. Process in agriculture.

Fig. 1 shows pre-harvest and post-harvest stages of crop-growing and smart farming practices. The first step is planting, which is followed by direct sowing or transplanting. Water levels are maintained via smart irrigation according to development stages. To guarantee a sufficient supply of water and lessen the load of field weeds, weed control is essential. This strategy lowers the cost of agriculture [12]. The monitoring of soil fertility is a crucial for maximizing plant development. In order to minimize losses, prompt and accurate identification of crop diseases and pest management are crucial. For example, categorizing, identifying, and forecasting

infestation patterns in fields are examples of operations included in the agricultural disease monitoring.

Analyzing crop growth utilizing vegetation, remotely sensed data, and climate variables is known as crop growth monitoring. There is also mapping of crop-growing zones at the field level. Vegetation indices, remotely sensed data, and hyper spectral data are used to estimate agricultural production. Harvesting, managing, organizing, cleaning, and transporting are examples of post-production jobs. The quality of crops may be assessed using machine learning techniques [13]. Activities like evaluating the crop's quality or looking into how climate change may affect crop production are frequently included in determining the crop's quality. The crop will next be dried using conventional or mechanical methods in the following stage of the process. The milling procedure, which eliminates the husk, is the final step in the post-production stage. Using image processing and machine learning methods, classification is to distinguish and categorize crop sample objects based on color and texture properties. Key contributions of this research are,

- **Advanced Sensing Technology Integration:** The research introduces a pioneering approach by utilizing Unmanned Aerial Vehicles (UAVs) equipped with hyper spectral sensors, showcasing the integration of cutting-edge sensing technologies for detailed spectral data collection in agricultural landscapes.
- **Precise Hyper spectral Data Processing:** The study emphasizes meticulous data pre-processing techniques, including radiometric calibration and geometric corrections using the Hyperspace program. This ensures the accurate conversion of digital data into radiance data, enabling the separation of mixed spectral signals associated with crops, soil types, and other agricultural variables.
- **Innovative CNN Framework for Feature Extraction:** The research employs a Convolutional Neural Network (CNN) framework to extract key features from hyper spectral data, such as NDVI, CCCI, CVI, contrast, and entropy indices. This innovative approach enhances insights into crop health and landscape dynamics, contributing to the field of precision agriculture.
- **Optimized CNN-LSTM Model for Crop Yield Prediction:** The study introduces a novel Optimized CNN-LSTM model for accurate crop yield prediction. By integrating deep learning with Firefly Algorithm optimization, the model leverages hyper spectral feature extraction through multiple hidden layers, showcasing a sophisticated and effective methodology for yield estimation.
- **Robust Evaluation Metrics and Validation:** Rigorous evaluation using metrics like R2, RMSE, MAE, and cosine similarity underscores the robustness and accuracy of the proposed Optimized CNN-LSTM model. The validation of the methodology's dependability provides confidence in the reliability of the findings, contributing to the advancement of agricultural remote sensing and predictive modelling.

Dataset In summary, the methodology combines advanced techniques from remote sensing, deep learning, and optimization to provide a comprehensive and effective approach for crop yield prediction and agricultural assessment. The contributions of this study have the potential to significantly impact precision agriculture by enabling farmers to make data-driven decisions for resource management and crop production. The remainder of this work is structured as follows: Section II offers a full analysis of these as well as related previous work. Details of the problem statement are included in Section III. In Section IV, the suggested Optimized CNN-LSTM architectures are covered in more depth. The results of the trials are discussed in Section V, and the proposed technique is thoroughly compared with existing best practices. Section VI concludes the paper.

II. RELATED WORKS

A predicted scientific approach is the integration of self-governing computing and artificial intelligence technology for agricultural ideas. With its extensive coverage, great spectral resolution, and wide range of narrow-band selection, the aerial hyperspectral system is a fantastic instrument for predicting crop physiological parameters and yield. It has been difficult to spread awareness of this technology due to the substantial and redundant three-dimensional analysis and computing. Based on three crop classifications with multi-functional cultivation, this research included two significant publicly available systems (R and Python), automatic hyperspectral narrow-band vegetation index estimation, and the most advanced machine learning (ML) modern equipment to calculate yield. Li et al.[14] demonstrated that AutoML regression model's predicted capacity was considerable. For single variety planting wheat, the best determination coefficient and normalized root mean square error (NRMSE) were 0.96 and 0.12, correspondingly; The restriction of the Auto-Sklearn approach, which prevents the investigation of the relevance ranking of individual feature, limits the capacity to retrace all regressors in this study, which may have an influence on the choice of appropriate vegetation indices.

Alfalfa is an important farmed feed crop. Due to effectiveness in data collecting, unmanned aerial vehicles (UAVs) are attracting in precision agriculture. hyperspectral data can provide a better level of spectral fidelity compared to other imaging techniques. Feng et al. [15] used UAV-based hyperspectral images, a feature selection is conducted to diminish the size of the data and retrieved a significant number of hyperspectral indices of the original image. Then, by merging three frequently used base learners, namely, support vector regression (SVR), K-nearest neighbors (KNN) and random forest (RF), an ensemble machine learning model was created. It demonstrated that ensemble model outperforms all base learners, and when employing the chosen features, an R_2 of 0.874 was obtained. The outcomes further support the effectiveness of the suggested ensemble model. The performance of the model might be affected by variables that were not taken into account for this research, such shifting field conditions, climatic variations, or insect infestations.

Artificial intelligence has easily migrated into a number of economic sectors, particularly for surveillance and control in

agriculture. One of the main factors reducing crop output is biotic stress. Albanese, Nardello, and Brunelli [16] proposed Automatic recognition of hassle using images has emerged as a key study area for timely crop disease diagnosis by the advent of deep learning technologies. In order to continuously identify infestations of pests inside fruit orchards. The embedded approach is built on sensor device. The platform's capabilities have been shown through the training and deployment of three distinct ML algorithms. Furthermore, the incorporation of energy-harvesting functions into the suggested system guarantees extended battery lifetime. One drawback of this research is that the energy harvesting system's effectiveness heavily relies on the availability of sufficient sunlight, making it less practical in regions with limited sunlight or during extended periods of overcast weather.

Weed growth out of control has a negative impact on crop quality and productivity. Herbicide usage to eradicate weeds changes biodiversity and pollutes the environment. Instead, pinpointing weed-infested areas can help with targeted chemical remediation of these areas. There are now ways to detect weed plants due to improvements in agricultural image analysis. Supervised learning techniques needs a massive volume of human annotated images. Because there are so many different plant species being grown, these supervised systems are therefore economically unviable for the small-scale farmer. In this research, Shore Wala et al. [17] present a semi-supervised deep learning method. This weed quantity and distribution may be helpful in autonomous robot-assisted targeted treatment of diseased regions. Convolutional Neural Network (CNN) is used to identify the foreground vegetation indices including crops and weeds. The requirement for manually developing features is therefore removed by utilising a fine-tuned CNN to identify the weed-infested areas. The method is tested on two datasets (1) images of carrot plants, and (2) the Sugar Beets dataset. The suggested approach has an optimal recall of 0.99 and an average accuracy of 82.13% for estimating weed density in weed-infested areas. The limitation of this work is time consuming.

Techniques for proximal sensing may be used to examine soil and crop factors that affect agricultural output. By combining this precision agricultural technology with cutting-edge data processing techniques like machine learning (ML) algorithms, it is possible to fully realize their promise for managing crop productivity. In order to forecast potato tuber yield, four machine learning (ML) algorithms, namely elastic net (EN), linear regression (LR), and support vector regression (SVR), k-nearest neighbor (k-NN) were employed by Abbas et al. [18]. Data of soil were sampled for soil chemistry, moisture content of the soil and normalized-difference vegetative index (NDVI). At the conclusion of the growing season, manual data collection and yield sample collection took place. The data from three fields were then combined to create four datasets, PE-2017, NB-2018, NB-2017 and PE-2018 which reflect the provincial data for the corresponding years. To develop yield projections evaluated using various statistical factors, modelling approaches were used. SVR models excelled all other models. The performance can be improved by using deep learning methods.

Crop supervision is changing as a result of neural networks and self-driving computers being integrated into agriculture. Crop production predictions are more accurately made thanks to overhead hyperspectral sensors and sophisticated predictive methods like combined models and AutoML regression. The accuracy of farming is improved by drones that operate using hyperspectral data; lucerne cultivation is one example of this. Using picture recognition and sensor devices, deep learning technologies facilitate the prompt identification of agricultural diseases. Promising results have been obtained using a semi-supervised deep learning approach to detect weeds, and machine learning methods are used to predict the yield of potato tubers depending on crop and soil characteristics. Even though these developments solve important issues, issues like consuming time and dependent on the climate energy collecting systems are still recognized.

III. PROBLEM STATEMENT

The existing methods may face limitations in feature ranking, energy availability for sensor devices [16], economic viability for small-scale farmers, time-consuming processes [17] and inefficient. To address these challenges, the proposed approach combines self-governing computing, hyperspectral feature extraction via Convolutional Neural Networks (CNN), and machine learning optimization techniques. Optimized CNN-LSTM model is introduced, integrating hyperspectral data analysis and yield prediction through multiple hidden layers. The model enhances performance through Firefly Algorithm optimization. This comprehensive approach contributes to accurate crop yield prediction, thereby improving precision agriculture practices.

IV. METHODOLOGY

This research capitalizes on Unmanned Aerial Vehicles (UAVs) equipped with hyperspectral sensors to meticulously capture intricate spectral data across agricultural terrains. The reliability and usability of the created models in actual agricultural contexts are ensured by modifying testing techniques to account for temperature, humidity, precipitation, and other meteorological parameters. Data preprocessing encompasses radiometric calibration and geometric corrections via the HyperSpec program, ensuring the precise conversion of original digital data into radiance data. Using NFINDR algorithm, mixed spectral signals in hyperspectral images are separated, revealing distinct fingerprints associated with crops, soil types, and agricultural variables. Integral to precision agriculture, a Convolutional Neural Network (CNN) framework extracts key features from hyperspectral data, including NDVI, CCCI, CVI, contrast, and entropy indices, heightening insights into crop health and landscape. A pioneering Optimized CNN-LSTM model is introduced for accurate crop yield prediction. Fusing deep learning employed with Firefly Algorithm optimization, the model integrates hyperspectral feature extraction, enabling precise yield estimation through multiple hidden layers. Rigorous evaluation, incorporating metrics like R^2 , RMSE, MAE, and cosine similarity, underscores the Optimized CNN-LSTM model's robustness and accuracy, thus validating the proposed methodology's dependability. It is illustrated in Fig. 2.

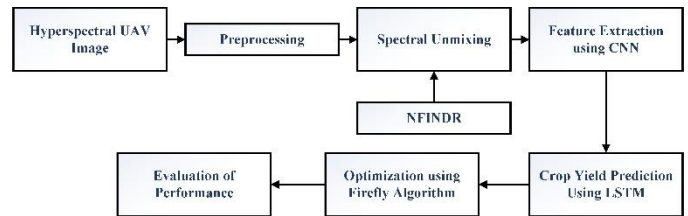


Fig. 2. Proposed model CNN-LSTM.

A. Data Collection and Preprocessing

Sensors attached on UAV flying over the countryside take hyperspectral images. Each pixel in the images has specific spectral characteristics [19]. The maker of the sensor used the HyperSpec program to perform radiometric calibrating and geometrical corrections on the UAV hyperspectral imagery. The sensor's laboratories evaluation factors, which may be represented as in Eq. (1), were used to convert the original digital number data into radiance data for the radiometric evaluation.

$$D_N = (R_1 G_1 + R_2 G_2) \times T_E + F_D \quad (1)$$

where, R_1 is the anticipated radiometric standard radiance for the first-order reflected image, R_2 is the radiometric standard radiance for the second-order reflected image, R_1 and R_2 's system gains are G_1 and G_2 , while the sensor's exposure time T_E is and the darkness of field measurement is F_D . Since the R_2 strength is so poor, a spectral filter may be used to filter it. In most cases, the calibration variables are determined by the producer using an integrated sphere in the lab, and they are then stored in the calibration program. According to a correlated equation, GPS (Global Positioning System) and also inertia measuring units (IMU) modules' location and orientation data, and other data, the geometric correction can be carried out. The input parameters for the HyperSpec program include the original hyperspectral information, its frame indices, timestamps, digital surface model (DSM) information, and the GNSS/IMU files containing yaw, pitch, roll, latitude, and longitude [20]. Further enhancing the precision of the geometric correction may be done by using ground control points (GCPs).

B. Spectral Unmixing using NFINDR Algorithm

The process of "spectral unmixing" is employed to separate the mixed spectrum signals generated by hyperspectral images to its constituent parts. This entails recognizing and isolating the spectral fingerprints of numerous factors in relation to farming, such as distinct crops, different kinds of soil, and sometimes even pests or illnesses that may be detected in the fields. The landscape's structure will benefit from knowing that data. Five distinct groups, containing soil, shadows, spikes, crop leaves and gray panels, were present in hyperspectral image data. Thus, each of these five groups can all contribute to the spectral sensitivity of a pixel to varying degrees and with somewhat different spectral signatures. Five endmembers, every indicating one group, were found from the images taken at five-meter height to show the large number of these categories of each pixel found in the images obtained at 20-meter height. When these images are made, the ensuing dataset mimics one that can be logically collected anyway. The NFINDR technique is used to execute spectral unmixing at the

subsequent step. The NFINDER approach is essentially an automated method for locating the cleanest pixels in a picture. The primary goal of this approach is to precisely replicate the effective (non-automated) method of locating the highest and lowest points of scatter chart. The convex structure of the available hyperspectral data makes it possible to use the NFINDER methodology in a reasonably simple and rapid manner. Endmembers = nfindr (inputData, numEndmembers, Name, Value) is a built-in MATLAB code that has been used in the suggested workflow. This function uses the NFINDER technique to obtain endmember signals out of hyperspectral data. The amount of endmember signatures to be retrieved with the NFINDER technique is denoted by numEndmembers. This form is employed when both reduction of dimensionality and parameters for the number of cycles are necessary. The extracted endmembers relate to certain soil constituents at specified wavelengths. For a variety of uses, such as crop detection and tracking in agriculture utilizing UAV-based hyperspectral imaging, the NFINDER technique has shown to be excellent for unmixing hyperspectral data efficiently on the computer [21].

C. NFINDER Algorithm

1) Minimize the incoming data's spectral dimensionality and estimate the primary component bands. Decide the quantity of PC wavelengths and endmembers will be extracted, and then extract that amount.

2) As a first group of endmembers, randomly select n pixel spectrum out of the minimized data.

3) Initialize iteration 1 and first collection of endmembers to determine the volume using $V(M^{(1)}) = |\det(M^{(1)})|$

$$\text{where, } M^{(1)} = \begin{bmatrix} 1 & 1 & \dots & 1 \\ m_1^{(1)} & m_2^{(1)} & \dots & m_p^{(1)} \end{bmatrix}$$

4) Choose a new pixel spectrum s, for this second cycle., such that: $s \notin \{m_1^{(1)}, m_2^{(1)}, \dots, m_p^{(1)}\}$.

5) Calculate the area of the resultant simplex $V(M^{(2)})$ after replacing all endmember of the collection with r.

6) If the calculated volume $V(M^{(2)})$ is higher than $V(M^{(1)})$, update the i^{th} endmember of the collection with r. A revised list of endmembers generated.

7) Choose a different pixel spectrum for each subsequent iteration, then repeat steps 5 and 6 with that new spectrum. Once the overall level of iterations reaches the desired number, the iterations come to an end.

D. Accuracy Prediction using Cosine Similarity

The accuracy for the spectral unmixing is assessed using cosine similarity as in Eq. (2), as well as it is also determined if the endmember frequencies acquired can be coincided with the wavelengths originally utilized to create the hyperspectral images.

$$\text{Similarity} = \cos(\theta) = ((E * P) / (\|E\| * \|P\|)) \quad (2)$$

where, $\| \cdot \|$ stands for the vector's magnitude (Euclidean norm), P is the vector representing each pixel's spectrum signature, and E is the chosen endmember option vector.

E. Extracted Features of Hyper Spectral Images using Convolutional Neural Network (CNN)

Precision agriculture, which applies resources like water, fertilizer, and pesticides especially when and where they are required, depends on the ability to extract features of hyperspectral crop images. Farmers may use resources more efficiently, cut down on waste, and boost crop output by having a better grasp of the variation in crop nutritional demands throughout a field. The features were extracted using CNN.

1) *Normalized Difference Vegetation Index (NDVI)*: NDVI represents the health and vigor of plants in an area. It is estimated as of the reflectance of two bands, typically the near-infrared (IR_N) and the red (R) bands, using the following Eq. (3).

$$NDVI = \frac{IR_N - R}{IR_N + R} \quad (3)$$

NDVI values range from -1 to +1, where positive values point to healthy vegetation, zero represents non-vegetated areas (e.g., water bodies), and negative values (closer to -1) typically represent cloud cover or man-made surfaces.

2) *Canopy Chlorophyll Content Index (CCCI)*: CCCI is another vegetation index used to estimate the chlorophyll content in vegetation canopies. It is particularly useful for monitoring the greenness and health of vegetation. The CCCI involves the red-edge band (R_E) is given in Eq. (4).

$$CCCI = \frac{IR_N - R_E}{IR_N + R_E} \cdot NDVI \quad (4)$$

Higher CCCI values indicate higher chlorophyll content and healthier vegetation.

a) *Chlorophyll VI (CVI)*: Chlorophyll VI is an index designed to provide a more accurate estimation of chlorophyll content in vegetation as in Eq. (5). It utilizes the red band (R), and the green band (G).

$$CVI = IR_N \times \frac{R}{G^2} \quad (5)$$

CVI values are positively correlated with higher chlorophyll content.

b) *Contrast*: Contrast is a statistical measure used to describe the difference in pixel intensities within an image or a specific region. In hyperspectral imagery, contrast refers to the variation in spectral values across different bands. Higher contrast indicates more pronounced differences between spectral signatures, which can be useful for discriminating between different materials or classes as shown in Eq. (6).

$$\text{contrast} = \sum_{k,l=1}^N P_{k,l} (k-l)^2 \quad (6)$$

c) *Entropy*: Entropy is another statistical measure that quantifies the amount of uncertainty or disorder in an image or a specific region as in Eq. (7). In hyperspectral images, entropy can be used to assess the complexity and variability of spectral signatures. High entropy values indicate greater spectral diversity and complexity, which can be helpful for identifying diverse land cover types.

$$Entropy = \sum_{k,l=1}^N P_{k,l} (\ln P_{k,l})^2 \quad (7)$$

NDVI, CCCI, and CVI are all vegetation indices that provide information about the health and vigor of crops. By calculating these indices from hyperspectral data, it becomes possible to monitor the growth status, stress levels, and overall health of crops [22].

F. Yield Estimation using LSTM

LSTM [23] By including a gradient superhighway in the structure of a state of a cell c as well to the hidden state h , a unique type of RNN was developed to address this problem. The LSTM architecture features gates that allow both the addition and removal of data from the cell state. The forget gate determines whether data should be eliminated from the current state of the cell and is described as follows:

$$f'_t = \sigma(W'_{f'} [h'_{t-1}, x'_t] + b'_f) \quad (8)$$

The definition of the input gate that chooses the data to be fed to the state of the cell is in Eq. (9).

$$i'_t = \sigma(W'_{i'} [h'_{t-1}, x'_t] + b'_{i'}) \quad (9)$$

Utilizing both and it, the cell state c'_t is derived in the way shown in Eq. (10).

$$\dot{c}'_t = \tanh(W'_{c'} [h'_{t-1}, x'_t] + b'_{c'}) \quad (10)$$

$$c'_t = \tanh(f'_{t'} [h'_{t-1}, x'_t] + i'_{t'} \dot{c}'_t) \quad (11)$$

The concealed and outgoing state o'_t of the LSTM, respectively, are specified as.

$$o'_t = \sigma(W'_{o'} [h'_{t-1}, x'_t] + b'_{o'}) \quad (12)$$

$$h_t = o'_{t'} \tanh(c_t) \quad (13)$$

Fig. 3 depicts the architecture of proposed CNN-LSTM model. Due to a more efficient gradient flow during back propagation, LSTM is more successful at simulating lengthy sequences than a straightforward RNN.

G. Optimization using Firefly Algorithm

An optimization approach was utilized to determine the parameters for which the cost function was minimized

throughout the training procedure. The variation in light intensity and the evolution of attraction serves as the two pillars of the firefly optimization approach. A measure of attraction is the intensity, which is connected to the objective function. The relative attractiveness (α) as judged by other fireflies fluctuates when the distance d_{ij} between fireflies i and j shifts. Light loses intensity as it moves farther away from its source due to air absorption. Additionally, as shown in Eq. (14), the attractiveness varies according to the degree of absorption and the brightness $I(d)$ varies in accordance with the inverse square law.

$$I(d) = \frac{I_s}{d^2} \quad (14)$$

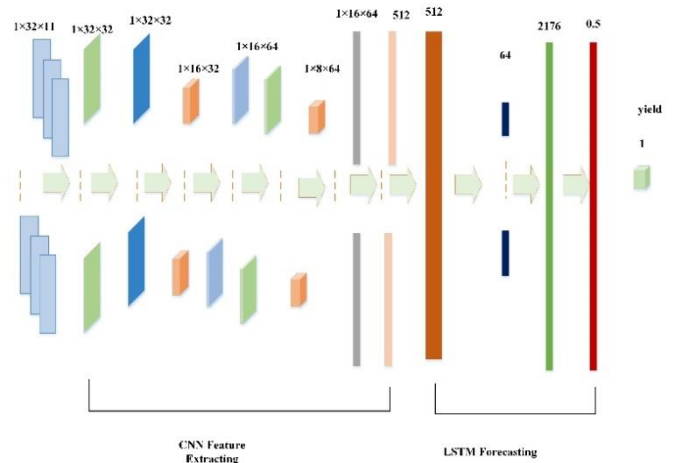


Fig. 3. The architecture of proposed CNN-LSTM model.

where, d is the distance between the source and the light, δ is the absorption coefficient of light, and I_s is the source intensity. Eq. (15) states that the light's intensity (I), which is dependent on its coefficient of absorption, varies with distance d .

$$I = I_0 e^{-\delta d^2} \quad (15)$$

where, I_0 is the initial brightness of the light, and $e^{-\delta d^2}$ is the sum of the intensities at the source and at a distance. The chosen attributes that each firefly location represents are used to assess the effectiveness of the crop Yield detecting model. Each firefly's attractiveness (α) in comparison to others is determined based on the fitness values received during the evaluation, as stated in Eq. (16).

$$\alpha = \alpha_0 e^{-\delta d^2} \quad (16)$$

Higher fitness values make fireflies attractive. After that, transport the firefly in that direction so they can explore the search area. To strike a balance between exploration and exploitation, adjust the Firefly Optimization algorithm's control parameters, such as the attraction coefficient, absorption coefficient, and iterations. Decide on the termination criteria, which govern when the optimization process should be stopped. Reaching a predetermined number of iterations or obtaining a good fitness value are frequent reasons for termination [24].

Algorithm 1: Firefly Algorithm

Initialize fireflies randomly
 Set control parameters (alpha, delta, iterations)
 Repeat for a predefined number of iterations:
 Calculate fitness values for each firefly
 Update the attractiveness (alpha) based on fitness and distance
 Move fireflies towards more attractive ones
 Explore the search space
 Until termination criteria met

V. RESULT AND DISCUSSION

Following is an explanation of how to test the accuracy of the CNN-LSTM model using the coefficient of determination (R²), mean absolute deviation (MAE), and root mean square error (RMSE):

A. Model Accuracy Assessment Parameters

To assess the accuracy of the yield prediction approach, the coefficient of determination (R²), mean absolute deviation (MAE), and root mean square error (RMSE) were utilized. R², MAE, and RMSE are calculated as in Eq. (17), Eq. (18) and Eq. (19).

$$R^2 = 1 - \frac{\sum_{k=1}^N (\hat{y}_k - y_k)^2}{\sum_{k=1}^N (y_k - \bar{y})^2} \tag{17}$$

$$RMSE = \sqrt{\frac{\sum_{k=1}^N (\hat{y}_k - y_k)^2}{N}} \tag{18}$$

$$MAE = \frac{1}{k} \sum_{k=1}^N |y_k - \hat{y}_k| \tag{19}$$

where, \bar{y} is the mean for the detected crop yield, y_k and \hat{y}_k are the observed and estimated crop yields, respectively; N represents the number of evaluation samples. A greater prediction performance of the model is shown by an increased R² and a decreased RMSE [25].

The assessment parameters for the Optimized CNN-LSTM model in Table I demonstrate its exceptional performance. The hyperspectral image dataset's underlying patterns are very well captured and understood by the model, as seen by the Coefficient of Determination (R²) value of 0.893, demonstrating the model's capacity to explain variations in observed data. Furthermore, the model's accuracy and dependability in predicting crop yields are shown by the low Root Mean Square Error (RMSE) of 0.13 and Mean Absolute Error (MAE) of 0.14. These findings demonstrate Optimized CNN-LSTM potential as a formidable tool for hyperspectral image-based yield forecasting, providing insightful information for remote sensing and precision agricultural applications. Fig. 4 depicts the Assessment parameter of Optimized CNN-LSTM.

B. Statistical Analysis

To investigate the impact of variation in breeds, irrigation methods, and their relations on the observed and anticipated crop yield, a mixture of linear model was used. The model's equation is given in Eq. (16).

$$Y = \alpha X + \gamma Z + e \tag{16}$$

where, X and Z stand for static effects and random effects accordingly, Y is the response shown by fixed effect (α) as well as random effect (γ) by a random error (e). With an interval from zero to one, broad-sense heritability measures the proportion of genetic variance to all phenotypic variation. The variance in phenotype is totally influenced by genetic and environmental variables, respectively, as indicated by the heritability of 0 and 1. The following Eq. (17) was used to compute the heritability.

$$h^2 = \frac{v_g}{(v_g + v_e/r)} \tag{17}$$

where, v_g and v_e stand for the genetic and erroneous variances, correspondingly, and r stands for the number of reproductions per treatment.

Table II presents the Coefficient of determination (R²) performance metrics for different predictive models. Random Forest (RF) achieved an R² value of 0.882, indicating a strong ability to explain the variance in the data. Support Vector Regression (SVR) performed well with an R² of 0.824, capturing a substantial portion of the data's variability. Optimized CNN-LSTM model exhibited the highest performance, attaining an R² of 0.893, signifying its superior capability in predicting and understanding the underlying patterns within the dataset. Fig. 5 shows comparison of various models with R².

TABLE I. ASSESSMENT PARAMETER OF OPTIMIZED CNN-LSTM

Assessment Parameters	Values
R2	0.893
RMSE	0.15
MAE	0.14

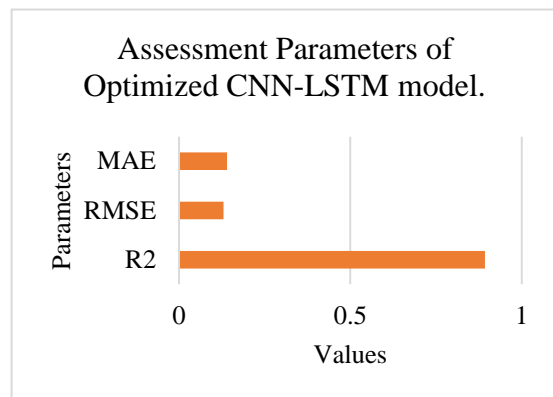


Fig. 4. Assessment parameter of optimized CNN-LSTM.

TABLE II. ACCURACY ASSESSMENT PARAMETER

Model	R ²
RF	0.882
SVR	0.824
Optimized CNN-LSTM	0.893

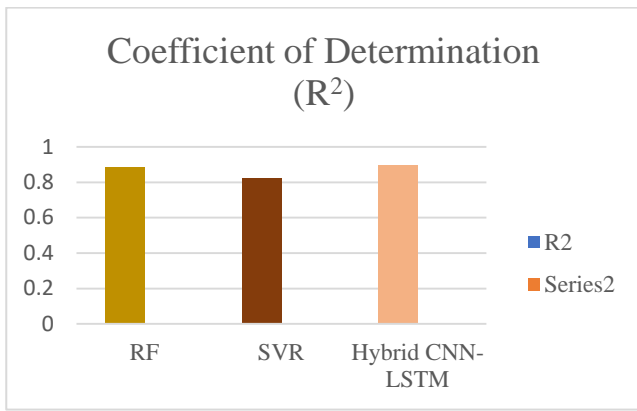


Fig. 5. Comparison of R^2 for various models.

Fig. 6 which depicts the training accuracy of proposed Optimized CNN-LSTM model. The accuracy model is plotted based on the value of R^2 . It clearly shows that the proposed method outperforms other algorithms.

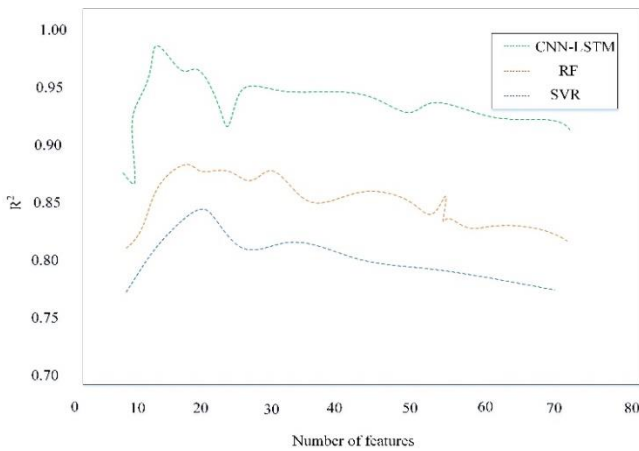


Fig. 6. Training accuracy with existing model.

This research used a dataset obtained from Unmanned Aerial Vehicles (UAVs) to analyze hyper spectral images in agricultural areas. The dataset was divided into two subsets for model development and evaluation. 80% of the dataset was allocated for the training phase, where the model learns patterns and relationships from the hyper spectral data. The remaining 20% was used for the testing phase, where the model encounters new data and evaluates its performance. This division is a standard practice in machine learning to gauge performance, prevent over fitting, and ensure reliability in real-world applications. The careful consideration of dataset partitioning is crucial for establishing the effectiveness and generalization of the developed models in agricultural hyper spectral image analysis. The training and test dataset were illustrated in Fig. 7.

The NFINDR algorithm is utilized to perform spectral unmixing on hyperspectral images. This technique separates mixed spectral signals into their constituent parts, identifying and isolating spectral fingerprints associated with different crops, soil types, and other factors relevant to agriculture. End members were selected as shown in Fig. 8.

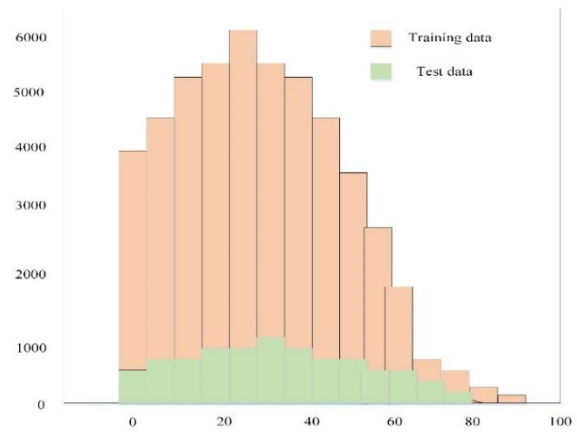


Fig. 7. Training and test dataset.

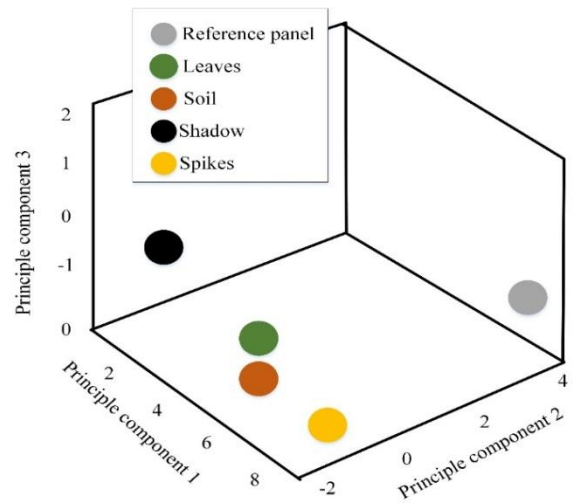


Fig. 8. Spectral unmixing using end members selection in NFINDR.

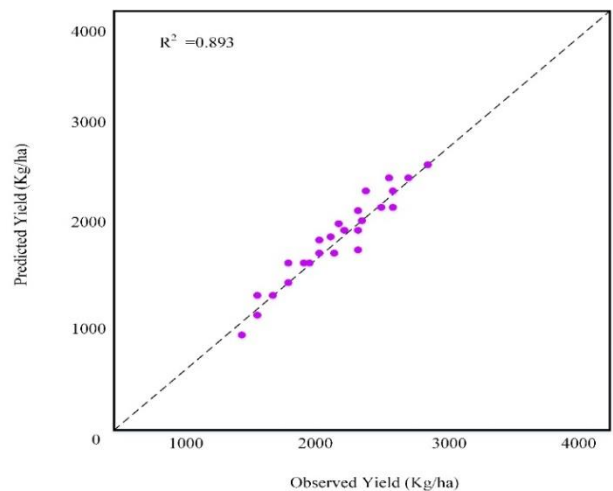


Fig. 9. The relation between observed and predicted yield with R^2 .

Fig. 9 depicts the relationship between observed and predicted yields with a coefficient of determination (R^2) value of 0.89. The data points closely follow a linear trend, indicating a link between the predicted and actual yields. The high R^2 value suggests that approximately 89% of the variability in the

observed yield can be explained by the predictive model, affirming its accuracy and reliability in forecasting agricultural yields. This alignment between predicted and observed values underscores the model's effectiveness in capturing the underlying patterns and factors influencing crop production.

Table III presents Root Mean Square Error (RMSE) values for different predictive models. The Random Forest (RF) model yielded an RMSE of 0.22, reflecting the average magnitude of prediction errors in relation to the observed values. The Support Vector Regression (SVR) model produced a slightly higher RMSE of 0.23, indicating a slightly greater overall error compared to RF. In contrast, the Optimized CNN-LSTM model demonstrated the lowest RMSE at 0.13, signifying its superior accuracy in predicting outcomes and minimizing prediction errors. These RMSE values provide insights into the precision and effectiveness of each model, with Optimized CNN-LSTM model emerging as the most precise in this analysis. The Training and testing loss is plotted based on RMSE value.

One of the most important aspects of this study's model evaluation is the training and validation loss analysis. The model's learning process and its capacity to generalize to new data are revealed by the plot of training and validation loss based on the Root Mean Square Error (RMSE) value. The model is effectively learning from the training data, indicating a successful training procedure, as seen by the decreasing trend in both training and validation loss. Given that there is little substantial divergence between the training and validation loss curves, it is possible that the model is not over fitting. This alignment shows that the model may generalize effectively to new, unexplored data points, increasing its dependability in real-world situations.

The model's accuracy and precision in forecasting crop yields are further supported by the low RMSE values linked to the training and validation loss, securing its application in remote sensing and precision agriculture settings. The training and testing loss expressed as RMSE is shown in Fig. 10.

Table IV showcases Mean Absolute Error (MAE) values for different predictive models. The Random Forest (RF) model achieved an MAE of 0.17. The Support Vector Regression (SVR) model exhibited a slightly lower MAE of 0.16, indicating a marginally improved accuracy in prediction compared to RF. Remarkably, Optimized CNN-LSTM model. Model outperformed the others with the lowest MAE of 0.14, underscoring its exceptional precision in forecasting and its ability to minimize absolute prediction errors. These MAE values provide valuable insights into the predictive capabilities of each model, with the Optimized CNN-LSTM model. It demonstrates the highest level of accuracy in this context.

The crop yield prediction models' accuracy was assessed using the accuracy assessment metrics coefficient of determination (R2), mean absolute deviation (MAE), and root mean square error (RMSE). The effectiveness of several prediction models, such as Random Forest (RF), Support Vector Regression (SVR), and Optimized CNN-LSTM model. It was evaluated using these measures. The outcomes showed that the Optimized CNN-LSTM model. It performed better than the competing models, earning the greatest R2 value of

0.893, demonstrating its improved capacity to account for the variance in the crop production data. Optimized CNN-LSTM model further demonstrated the lowest RMSE and MAE values at 0.13 and 0.14, respectively, emphasizing its outstanding accuracy in predicting crop yields. These findings highlight the value of combining deep learning, spectrum unmixing, and hyperspectral imaging in precision agriculture, with Optimized CNN-LSTM model demonstrating the most promising outcomes. The observed and projected yield connection, which has an R2 value of 0.89 and indicates that almost 89% of the variability in observed yield can be explained by the predictive model, provided more evidence of the model's accuracy. With useful insights for large-scale farming operations, this research shows the potential of cutting-edge technology and machine learning approaches to improve crop output estimates.

TABLE III. ROOT MEAN SQUARE ERROR (RMSE)

Model	RMSE
RF	0.22
SVR	0.23
Optimized CNN-LSTM	0.15

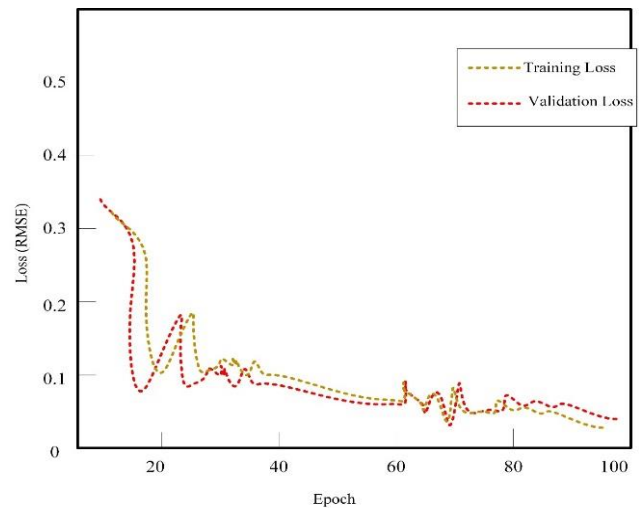


Fig. 10. Training and validation loss.

TABLE IV. MAE VALUES COMPARISON

Model	MAE
RF	0.17
SVR	0.16
Optimized CNN-LSTM	0.14

C. Discussion

The integration of self-governing computing and artificial intelligence in agriculture, particularly in crop monitoring and yield prediction, shows promise. Utilizing aerial hyper spectral systems and UAVs, combined with advanced machine learning techniques, improves crop yield predictions. Examples include AutoML regression models for wheat and an ensemble model for alfalfa. Deep learning technologies are used for disease identification and semi-supervised weed detection. Despite challenges like time-consuming processes and climate-

dependent energy-harvesting systems, the adoption of neural networks and precision agriculture technologies is transforming crop management.

VI. CONCLUSION AND FUTURE WORK

The suggested model combines deep learning, spectral unmixing, and hyper spectral imaging in a way that improves upon earlier methods for projecting crop production. As opposed to traditional methods that depend on subjective evaluations, this new approach makes use of hyper spectral photography to gather copious amounts of non-visible data, which enables a thorough analysis of crop characteristics. Spectral unmixing methods allow for the accurate assessment of crop health and growth stages by identifying distinct spectral signatures. This improved spectral data is then used by deep learning algorithms to create a solid, data-driven basis for precise crop production forecasts. A model with the lowest Root Mean Square Error (RMSE) of 0.15 and Mean Absolute Error (MAE) of 0.14 is produced by integrating these cutting-edge approaches with MATLAB, demonstrating improved prediction accuracy over existing models. This novel strategy overcomes the drawbacks of traditional approaches and greatly improves crop output forecast capabilities, marking a significant advance in precision agriculture. Future research in precision agriculture ought to concentrate on improving data integration by investigating the fusion of various sensors, IoT devices, and remote sensing technologies to capture a thorough dataset for crop monitoring. In order to provide openness and confidence in yield projections, explainable AI models also need to be developed.

REFERENCES

- [1] M.-L. Tseng, A. S. F. Chiu, C.-F. Chien, and R. R. Tan, "Pathways and barriers to circularity in food systems," *Resour. Conserv. Recycl.*, vol. 143, pp. 236–237, Apr. 2019, doi: 10.1016/j.resconrec.2019.01.015.
- [2] P. K. Sethy, C. Pandey, Y. K. Sahu, and S. K. Behera, "Hyperspectral imagery applications for precision agriculture - a systemic survey," *Multimed. Tools Appl.*, vol. 81, no. 2, pp. 3005–3038, Jan. 2022, doi: 10.1007/s11042-021-11729-8.
- [3] G. Avola, A. Matese, and E. Riggi, "An Overview of the Special Issue on 'Precision Agriculture Using Hyperspectral Images,'" *Remote Sens.*, vol. 15, no. 7, p. 1917, Apr. 2023, doi: 10.3390/rs15071917.
- [4] T. B. Shahi, C.-Y. Xu, A. Neupane, and W. Guo, "Machine learning methods for precision agriculture with UAV imagery: a review," *Electron. Res. Arch.*, vol. 30, no. 12, pp. 4277–4317, 2022, doi: 10.3934/era.2022218.
- [5] N. Sulaiman, N. N. Che'Ya, M. H. Mohd Roslim, A. S. Juraimi, N. Mohd Noor, and W. F. Fazlil Ilahi, "The Application of Hyperspectral Remote Sensing Imagery (HRSI) for Weed Detection Analysis in Rice Fields: A Review," *Appl. Sci.*, vol. 12, no. 5, p. 2570, Mar. 2022, doi: 10.3390/app12052570.
- [6] M. Ruiz, M. J. Beriain, M. Beruete, K. Insausti, J. M. Lorenzo, and M. V. Sarriés, "Application of MIR Spectroscopy to the Evaluation of Chemical Composition and Quality Parameters of Foal Meat: A Preliminary Study," *Foods*, vol. 9, no. 5, p. 583, May 2020, doi: 10.3390/foods9050583.
- [7] H. J. Escalante, S. Rodríguez-Sánchez, M. Jiménez-Lizárraga, A. Morales-Reyes, J. De La Calleja, and R. Vazquez, "Barley yield and fertilization analysis from UAV imagery: a deep learning approach," *Int. J. Remote Sens.*, vol. 40, no. 7, pp. 2493–2516, Apr. 2019, doi: 10.1080/01431161.2019.1577571.
- [8] B. Verma, R. Prasad, P. K. Srivastava, P. Singh, A. Badola, and J. Sharma, "Evaluation of Simulated AVIRIS-NG Imagery Using a Spectral Reconstruction Method for the Retrieval of Leaf Chlorophyll Content," *Remote Sens.*, vol. 14, no. 15, p. 3560, Jul. 2022, doi: 10.3390/rs14153560.
- [9] B. Lu, P. Dao, J. Liu, Y. He, and J. Shang, "Recent Advances of Hyperspectral Imaging Technology and Applications in Agriculture," *Remote Sens.*, vol. 12, no. 16, p. 2659, Aug. 2020, doi: 10.3390/rs12162659.
- [10] C. Sun et al., "Prediction of End-Of-Season Tuber Yield and Tuber Set in Potatoes Using In-Season UAV-Based Hyperspectral Imagery and Machine Learning," *Sensors*, vol. 20, no. 18, p. 5293, Sep. 2020, doi: 10.3390/s20185293.
- [11] J. Nalepa, "Recent Advances in Multi- and Hyperspectral Image Analysis," *Sensors*, vol. 21, no. 18, p. 6002, Sep. 2021, doi: 10.3390/s21186002.
- [12] S. A. Bhat and N.-F. Huang, "Big Data and AI Revolution in Precision Agriculture: Survey and Challenges," *IEEE Access*, vol. 9, pp. 110209–110222, 2021, doi: 10.1109/ACCESS.2021.3102227.
- [13] C. Nguyen, V. Sagan, M. Maimaitiyiming, M. Maimaitijiang, S. Bhadra, and M. T. Kwasniewski, "Early Detection of Plant Viral Disease Using Hyperspectral Imaging and Deep Learning," *Sensors*, vol. 21, no. 3, p. 742, Jan. 2021, doi: 10.3390/s21030742.
- [14] K.-Y. Li et al., "Toward Automated Machine Learning-Based Hyperspectral Image Analysis in Crop Yield and Biomass Estimation," *Remote Sens.*, vol. 14, no. 5, p. 1114, Feb. 2022, doi: 10.3390/rs14051114.
- [15] L. Feng et al., "Alfalfa Yield Prediction Using UAV-Based Hyperspectral Imagery and Ensemble Learning," *Remote Sens.*, vol. 12, no. 12, p. 2028, Jun. 2020, doi: 10.3390/rs12122028.
- [16] A. Albanese, M. Nardello, and D. Brunelli, "Automated Pest Detection with DNN on the Edge for Precision Agriculture," *IEEE J. Emerg. Sel. Top. Circuits Syst.*, vol. 11, no. 3, pp. 458–467, Sep. 2021, doi: 10.1109/JETCAS.2021.3101740.
- [17] S. Shorewala, A. Ashfaque, R. Sidharth, and U. Verma, "Weed Density and Distribution Estimation for Precision Agriculture Using Semi-Supervised Learning," *IEEE Access*, vol. 9, pp. 27971–27986, 2021, doi: 10.1109/ACCESS.2021.3057912.
- [18] F. Abbas, H. Afzaal, A. A. Farooque, and S. Tang, "Crop Yield Prediction through Proximal Sensing and Machine Learning Algorithms," *Agronomy*, vol. 10, no. 7, p. 1046, Jul. 2020, doi: 10.3390/agronomy10071046.
- [19] Y. Zhong, X. Hu, C. Luo, X. Wang, J. Zhao, and L. Zhang, "WHU-Hi: UAV-borne hyperspectral with high spatial resolution (H2) benchmark datasets and classifier for precise crop identification based on deep convolutional neural network with CRF," *Remote Sens. Environ.*, vol. 250, p. 112012, Dec. 2020, doi: 10.1016/j.rse.2020.112012.
- [20] A. Vinci, R. Brigante, C. Traini, and D. Farinelli, "Geometrical Characterization of Hazelnut Trees in an Intensive Orchard by an Unmanned Aerial Vehicle (UAV) for Precision Agriculture Applications," *Remote Sens.*, vol. 15, no. 2, p. 541, Jan. 2023, doi: 10.3390/rs15020541.
- [21] K. Lavanya, R. Jaya Subalakshmi, T. Tamizharasi, L. Jane, and A. Victor, "Unsupervised Unmixing and Segmentation of Hyper Spectral Images Accounting for Soil Fertility," *Scalable Comput. Pract. Exp.*, vol. 23, no. 4, pp. 291–301, Dec. 2022, doi: 10.12694/scpe.v23i4.2031.
- [22] W. Yang et al., "Estimation of corn yield based on hyperspectral imagery and convolutional neural network," *Comput. Electron. Agric.*, vol. 184, p. 106092, May 2021, doi: 10.1016/j.compag.2021.106092.
- [23] S. Sharma, S. Rai, and N. C. Krishnan, "Wheat crop yield prediction using deep LSTM model," *ArXiv Prepr. ArXiv201101498*, 2020.
- [24] N. Kardani, A. Bardhan, P. Samui, M. Nazem, A. Zhou, and D. J. Armaghani, "A novel technique based on the improved firefly algorithm coupled with extreme learning machine (ELM-IFF) for predicting the thermal conductivity of soil," *Eng. Comput.*, vol. 38, no. 4, pp. 3321–3340, Aug. 2022, doi: 10.1007/s00366-021-01329-3.
- [25] S. Fei, L. Li, Z. Han, Z. Chen, and Y. Xiao, "Combining novel feature selection strategy and hyperspectral vegetation indices to predict crop yield," *Plant Methods*, vol. 18, no. 1, p. 119, Nov. 2022, doi: 10.1186/s13007-022-00949-0.